*Protein Science* (1998), 7:2099–2105. Cambridge University Press. Printed in the USA.


# Crystal structure of spinach plastocyanin at 1.7 Å resolution

YAFENG XUE,[1,2] MATS ÖKVIST,[1] ÖRJAN HANSSON,[1] AND SIMON YOUNG[1]

[1]Department of Chemistry, Biochemistry and Biophysics, Göteborg University, P.O. Box 462, S-405 30 Göteborg, Sweden
[2]Astra Structural Chemistry Laboratory, S-431 83 Mölndal, Sweden

(RECEIVED March 26, 1998; ACCEPTED June 29, 1998)

**Abstract**

The crystal structure of plastocyanin from spinach has been determined using molecular replacement, with the structure of plastocyanin from poplar as a search model. Successful crystallization was facilitated by site-directed mutagenesis in which residue Gly8 was substituted with Asp. The region around residue 8 was believed to be too mobile for the wild-type protein to form crystals despite extensive screening. The current structure represents the oxidized plastocyanin, copper (II), at low pH (≈4.4). In contrast to the similarity in the core region as compared to its poplar counterpart, the structure shows some significant differences in loop regions. The most notable is the large shift of the 59–61 loop where the largest shift is 3.0 Å for the $C_\alpha$ atom of Glu59. This results in different patterns of electrostatic potential around the acidic patches for the two proteins.

**Keywords:** crystal structure; molecular replacement; rational engineering for crystallogenesis; spinach plastocyanin

Plastocyanin (Pc) is a soluble electron carrier in the photosynthetic electron-transfer chain of all higher plants as well as in a number of green algae and cyanobacteria. Its role is to transport electrons from the membrane-bound cytochrome $b_6f$ complex to P700, the reaction-center chlorophyll of the equally membrane-bound photosystem 1 (Gross, 1993; Redinbo et al., 1994).

The first crystal structure of poplar Pc (Colman et al., 1978) showed an overall fold of a $\beta$-barrel, consisting of two $\beta$-sheets with a total of eight strands. The copper ion is buried ≈6 Å from the surface of the "northern" end of the protein, where a highly hydrophobic patch with a number of conserved residues is located. The copper ligands, His37, Cys84, His87, and Met92, are completely conserved in all studied plastocyanins. Furthermore, there are a number of negatively charged residues constituting the so-called acidic patches on the "eastern" side of the protein from all higher plants. Both the hydrophobic and the acidic areas have been suggested to be of relevance to electron transfer. Using mutagenesis a large range of mutations have been introduced into both the hydrophobic patch, the acidic patches as well as the Tyr83, the residue that may play an important role in the electron transfer between Pc and cytochrome *f* (Young et al., 1997 and references therein).

Since the initial structure solution of oxidized poplar Pc, the apo form, the mercury-substituted protein and the reduced form at six different pHs, as well as the plastocyanins from two plants (French bean and parsley), three green algae (*Enteromorpha prolifera*, *Chlamydomonas reinhardtii* and *Scenedesmus obliquus*) and one blue-green algae (*Anabena variabilis*) have been determined, using X-ray crystallography and NMR (Bagby et al., 1994; Redinbo et al., 1994 and references therein; Badsberg et al., 1996). Recently, the crystal structure of a triple mutant Pc from the blue-green algae *Synechocystis* sp. PCC 6803 has also been reported (Romero et al., 1998).

Ever since investigations on Pc began, the favorite source of the protein has been spinach, since it is relatively easy to prepare the protein from this plant. In addition, its reaction partners in vivo, photosystem 1 and cytochrome $b_6f$, are often prepared from spinach. Therefore, numerous attempts have been made by us and others to crystallize wild-type spinach Pc, but with very limited success (Chapman et al., 1977). Instead, one has been forced to use the sequence homology with Pc from other sources, mainly the poplar protein that shares about 78% identity with the spinach protein, in discussions of structural aspects of spinach Pc. After having made a study of the intermolecular interactions in the crystal of poplar Pc, we exchanged a glycine in position 8 for an aspartic acid, attempting to stabilize a loop on the protein surface containing three glycines and in this way mimic the poplar protein. Here we report the first crystal structure of the spinach Pc at 1.7 Å resolution, and compare it to the structure of the oxidized poplar protein at 1.33 Å resolution (Guss et al., 1992).

## Results and discussion

### *Crystallization*

After extensive screening experiments, crystallization trials on the wild-type protein remained unsuccessful. Site-directed mutagen-

Reprint requests to: Yafeng Xue, Astra Structural Chemistry Laboratory, S-431 83 Mölndal, Sweden; e-mail: Yafeng.Xue@hassle.se.astra.com.

*Abbreviation:* Pc, plastocyanin.

esis was then used to facilitate the crystallization. The available crystal structures of the poplar protein were examined and surface regions involved in crystal packing interactions were identified. Sequence alignment of the poplar and spinach Pc was used to spot potential regions where mutations could be introduced to mimic the poplar protein and affect the crystal packing interactions. A region identified in this manner included amino acid residue 8. In spinach Pc a stretch of three glycines, from residue 6 to 8, makes it plausible that this region possesses a high degree of flexibility in the peptide chain, which may introduce heterogeneity in its conformation. Heterogeneity is believed to be a frequent cause of difficulties in crystallization. Therefore, as a first attempt to improve crystallization, a point mutation was introduced at position 8 to substitute glycine with aspartic acid.

Using a screening procedure, it was found possible to grow X-ray quality crystals of the mutant protein by the method described in Materials and methods.

*Expression and purification*

Despite the fact that the Gly8Asp mutation introduces an extra negative charge on the protein (above or near neutral pH), this mutant behaves as the wild-type protein in expression and purification. After the last ion-exchange column, an optical spectrum was taken to obtain the absorbance ratio $A_{277}/A_{597}$, which is used as a measure of the purity of the sample. The ratio for the mutant was 1.2, which is close to the determined value of 1.0 for the wild-type protein (Ejdebäck et al., 1997).

*Biochemical and biophysical characterization*

The isoelectric point was determined to be 3.55 (an average of three runs). This is at the lower limit of the useful pH range of the gel, so it should be treated with caution. The p*I* value for the wild-type, which was run in parallel to the mutant, was determined to be 3.82. This value agrees well with what has been reported previously (Sigfridsson et al., 1996). The program PCGENE was used to obtain theoretical estimates of 4.08 and 3.99 for the wild-type and mutant protein, respectively (Sigfridsson et al., 1996).

Spectral and kinetic characterization of the mutant and comparisons with the characteristics of the wild-type protein have been performed (Sigfridsson et al., 1997). As both the UV-vis and EPR spectra were similar to the wild-type, it was concluded that no significant disturbances had occurred at the copper site. Though there was a slight increase (20%) in the intracomplex electron-transfer rate constant from the mutant to P700 and a small shift toward the inactive complex, the mutant still showed biphasic kinetics, similar to the wild-type.

The reduction potential of the mutant protein was found to be decreased by at most 5 mV from the wild-type value of 384 mV.

*Quality of the model*

The structure of spinach Pc has been determined at a resolution of 1.7 Å with a final crystallographic *R*-factor of 0.183. (The coordinates have been deposited with the Brookhaven Protein Data Bank, ID code: 1AG6.) The refinement parameters and statistics have been summarized in Table 1. The current model contains 737 protein atoms, 1 copper atom, and 64 solvent molecules. The RMS deviation (RMSD) in bond and angle distances are 0.01 Å ($\sigma$ = 0.02 Å) and 0.03 Å ($\sigma$ = 0.04 Å), respectively. The RMSD from planarity is 0.01 Å ($\sigma$ = 0.03 Å) for peptide planes and 0.01 Å ($\sigma$ = 0.02 Å) for aromatic groups. Coordinate errors were estimated to be 0.18 Å by the Luzzati method. The geometry of the final model is very satisfactory as judged from PROCHECK (Laskowski et al., 1993): 91.2% (8.8%) of the residues fall into the most favored (additional allowed) regions in a Ramachandran plot (not shown). $R_{free}$ was used throughout the refinement to monitor the convergence and to prevent overfitting of the model. The average *B*-factor of the model is 23.7 Å$^2$, very close to the value of 22.8 Å$^2$, estimated from a Wilson plot (French & Wilson, 1978). The average *B*-factor over all main (side) chain atoms is 22.3 (25.2) Å$^2$. The solvent molecules have a mean *B*-value of 41.4 Å$^2$. The RMSD in *B*-values is 1.5 Å$^2$ ($\sigma$ = 2.0 Å$^2$) for the main chain and 2.1 Å$^2$ ($\sigma$ = 2.0 Å$^2$) for the side-chain bonds. Despite the relatively high *B*-factor, all the protein atoms have well-defined electron density in the $2F_o - F_c$ Fourier map, except three lysine residues, Lys54, Lys77, and Lys95, whose side chains are exposed to the solvent and for which only very weak density can be seen beyond $C_\delta$ atoms. Some aromatic side chains (Phe14, Phe29, Tyr70, Tyr83) show well-defined holes in their phenyl rings (Fig. 1). No significant extra peaks are found in the $F_o - F_c$ map (contoured at 3.5$\sigma$) calculated after the final refinement cycle.

**Table 1.** *Refinement parameters and statistics*

| | Data 2 |
|---|---|
| Number of atoms | 802 |
| Protein | 737 |
| Copper ion | 1 |
| Solvent | 64 |
| Number of parameters | 3,208 |
| Coordinate error estimation | |
| Luzzati method | 0.18 Å |
| Average *B*-factors | |
| All protein atoms | 23.7 Å$^2$ |
| Main-chain atoms | 22.3 Å$^2$ |
| Side-chain atoms | 25.2 Å$^2$ |
| Solvent atoms | 41.4 Å$^2$ |
| $R^a/R_{free}$ | 0.183/0.204 |

[a] $R = \Sigma_{hkl}(|F_o - F_c|)/\Sigma_{hkl}|F_o|$, $|F_o|$ and $|F_c|$ are observed and calculated structure factor amplitudes, respectively.

*The overall structure/crystal packing interactions*

The structure of spinach Pc is very similar to that of the poplar Pc. The core of the protein retains the well-defined $\beta$-barrel structure, as depicted in Figure 2A. Upon superposition of the present structure to that of the poplar (Protein Data Bank, entry code: 1plc) structure, the RMS distance between the $C_\alpha$ atoms is 0.696 Å. Significant displacement in backbone atoms was observed for the 59–61 loop where the largest shift is 3.0 Å for the $C_\alpha$ of Glu59. The side chain of Glu59 is pointing away from the position adopted in the poplar structure. Furthermore, the 59–61 loop region is involved in numerous crystal packing interactions in the spinach structure. Strong hydrogen bonding interactions were observed between the pairs of carboxylate oxygens of the Glu59 in one molecule and Asp61 from the neighboring molecule. One of these two carboxylates should be protonated to donate a proton in the

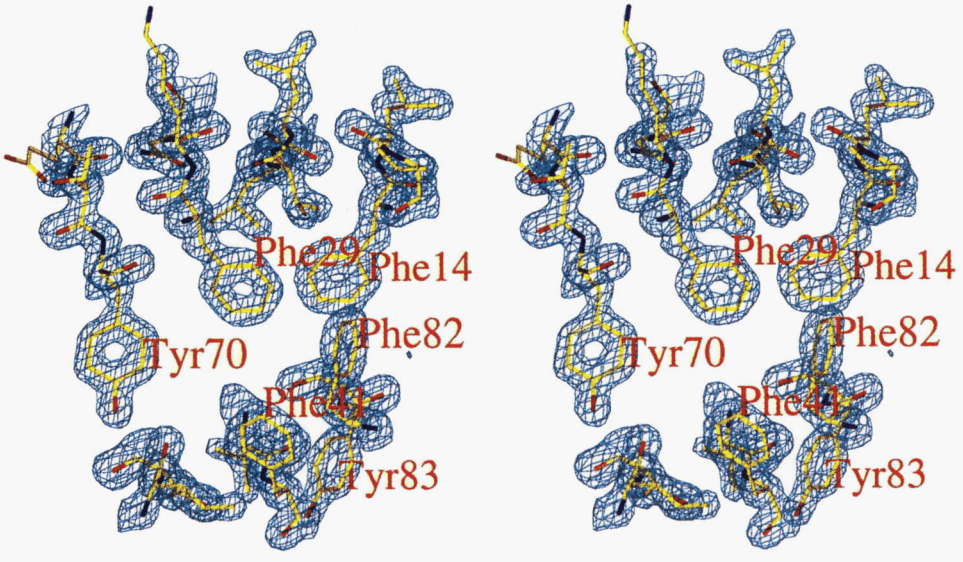


**Fig. 1.** Electron density map ($2F_o - F_c$), contoured at $1.5\sigma$, showing well-defined holes in the phenyl rings of Phe14, Phe29, and Tyr70. Plot produced with O/oplot (Jones et al., 1991).

hydrogen-bond. This is consistent with the fact that the crystal was grown at pH 4.4, which is very close to the p$K_a$ of the side-chain carboxylates of Asp and Glu (both have a p$K_a$ close to pH 4.7). In contrast, very few packing interactions were found in the corresponding region in the poplar Pc and the green alga, *C. reinhardtii* (Protein Data Bank, entry code: 2plt), structure (Redinbo et al., 1993), where only two and one hydrogen bonds, respectively, were found between molecules in the two structures. One internal water molecule is found in the protein. It is located in the southern end of the molecule where it provides a hydrogen-bonding bridge be-

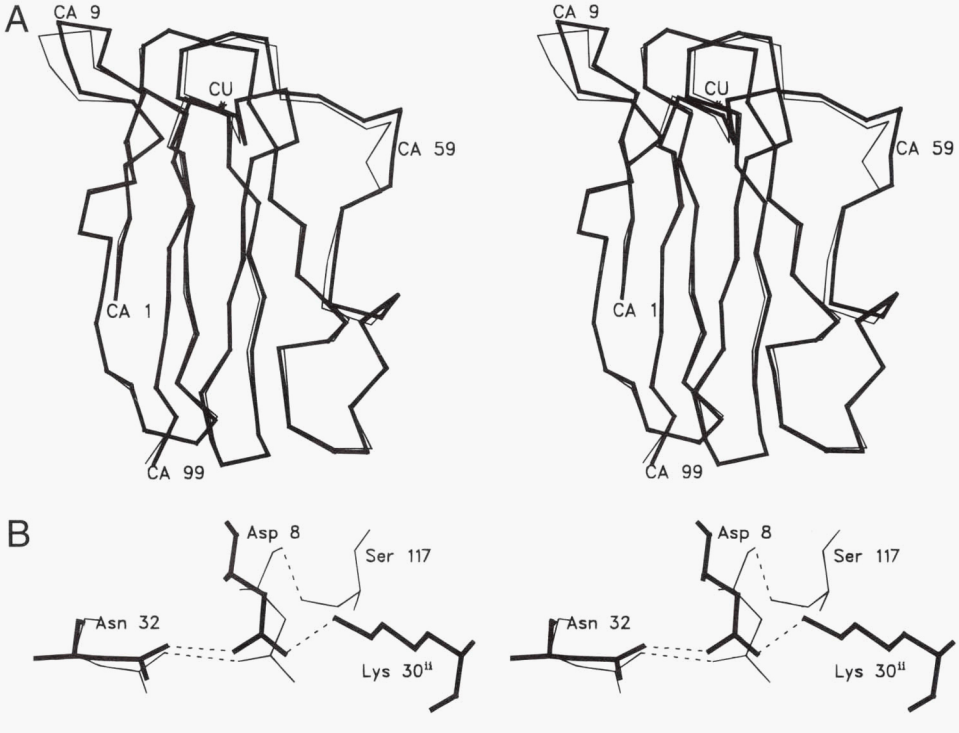


**Fig. 2.** Superposition of Gly8Asp spinach Pc (thick lines) and poplar Pc (thin lines). **A:** $C_\alpha$ traces. **B:** Illustration of the similarities in intramolecular contacts, and the differences in intermolecular contacts, for Asp8 in the mutant spinach Pc and poplar Pc. Plots produced with Setor (Evans, 1993).

tween the carbonyl oxygen of Glu25 and the amide nitrogen of Leu74. For the poplar structure two internal water molecules have been reported close to this position, as well as near residues 21, 25, and 27 (Guss et al., 1992).

The structure of the wild-type Pc from spinach has recently been determined by NMR (Bergkvist et al., pers. comm.). In this particular structure, the average position of the 59–61 region is even further dislocated from the observed position of this region in the X-ray structure of the poplar protein, compared to what is observed in the X-ray structure of the Gly8Asp mutant. It is possible that the observed conformation in this region results from crystal packing interactions. On the other hand, it is also possible that the orientation of the 59–61 loop in the spinach crystal structure may represent one of the possible native conformations if this region can indeed adopt multiple (discrete) conformations.

### *The effect of the mutation on the structure*

The loop around the mutated residue Asp8 shows significant shifts compared to the poplar structure. Such differences may be ascribed to differences in crystal contacts. However, in the mutant spinach Pc, Asp8 has the same intramolecular interaction as in the poplar structure, its side chain making a hydrogen bond with Asn32. In addition, the side chain of the Asp8 residue in spinach Pc is also involved in crystal packing interactions by forming hydrogen bonds to Lys30 of a neighboring molecule. In the poplar structure Asp8 is also involved in crystal packing, but via a hydrogen bond from the carbonyl oxygen to the side chain of Ser17 instead (Fig. 2B).

### *The copper site*

The copper site is located in the northern end of the molecule, between the loops that connect the $\beta$-strands. The oxidized copper ion is coordinated by the $S^{\gamma}$ atom of Cys84, the $S^{\delta}$ atom of Met92 and the $N^{\delta 1}$ atoms of His37 and His87. The geometry of the copper site shows no significant difference compared to that of the poplar protein. The largest differences between the two copper sites is observed in the distances between the copper atom and the $N^{\delta 1}$ atoms of the histidines His37 and His87. These differences, 0.11 and 0.16 Å, respectively, are small compared to the estimated overall error of the coordinates of the spinach structure.

An interesting observation is that small residual densities are visible around the copper in the difference map, contoured at $3\sigma$. This can often be the result of errors not accounted for during data collection/reduction, e.g., absorption caused by the nonregular shape of the crystal and/or nonisotropic scattering of the crystal. Although further refinement using REFMAC, which included anisotropic scaling, did significantly reduce the residual density around the copper, some residual density is still visible, mainly between the Cu and the $S^{\gamma}$ of Cys84, and between the Cu and the $S^{\delta}$ of Met92. Assuming that such residual densities indeed reflect the local disorder of the molecule, it can be attributed to either static or thermal disorder. It is often difficult in crystallographic analysis to differentiate between these two types of disorder. It has recently been demonstrated that time-differential perturbed angular correlation spectra of $^{111m}$Cd-derivatives of spinach Pc exhibit a peculiar line profile. The observation was interpreted as a small scale flexibility within the trigonal plane of the metal center. This occurs in Pc, but not in other copper proteins such as azurin, stellacyanin, ascorbate oxidase, or laccase (Tröger et al., 1996). The residual densities around the copper that are observed in the present investigation may be related to this flexibility. Superposition of the spinach structure and the structure of poplar protein in the reduced form at pH 3.8, indicated that the copper position in the reduced form is in close overlap to the residual density in the $F_o - F_c$ map. Since the present spinach structure is from a crystal grown and maintained at pH 4.4, it cannot be ruled out that some static disorder; for example, a small portion of protein with reduced copper also contributes to the observed residual density.

### *The protein surface*

Numerous studies, based on chemical and genetical modifications, address the question of which amino acid residues on the surface of Pc are important for the interaction with redox partners. Both electrostatic and dynamic properties have been found to be important. Figure 3 compares the electrostatic potential at the solvent-accessible surface of the spinach and poplar proteins. The positive potential at the hydrophobic surface is mostly due to the oxidized copper ion whose charge is only partly neutralized by the thiolate ligand (Fig. 3A,B). The potential at this patch becomes essentially zero upon reduction of the copper ion (Durell et al., 1990).

The acidic patches give rise to large areas of negative potential whose extent differs between the two proteins. There is a clear separation of the upper and lower acidic patches for the spinach protein, which is not seen for the poplar protein (Fig. 3C,D). This discrepancy, which arises from differences in the conformations of the side chains (see the Crystal packing interactions section) and not in their chemical identity, could be of importance in the binding to the redox partners. However, the acidic patches are quite

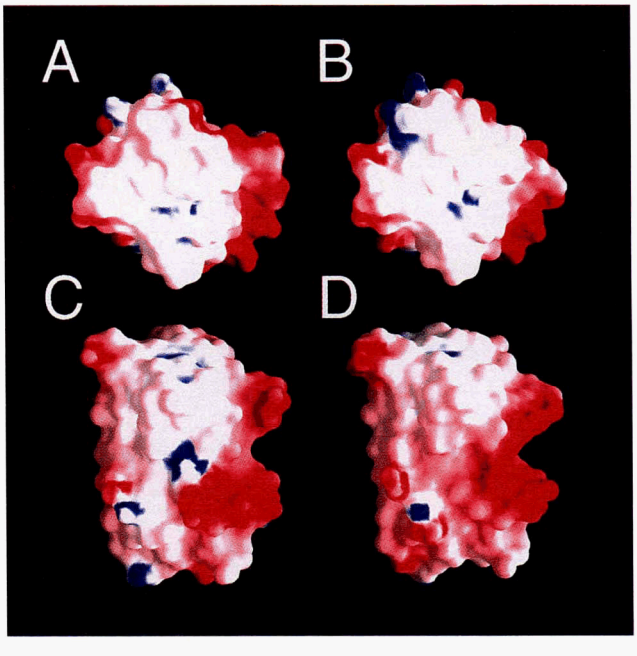


**Fig. 3.** Electrostatic potential at the solvent-accessible surface of Gly8Asp spinach Pc (**A**, **C**) and poplar Pc (**B**, **D**). The region around the hydrophobic patch is shown in **A** and **B** and the acidic patches are shown in **C**, **D**. Color scale: red, white, blue for negative, no, and positive potential, respectively. The plots were produced by GRASP (Nicholls et al., 1991).

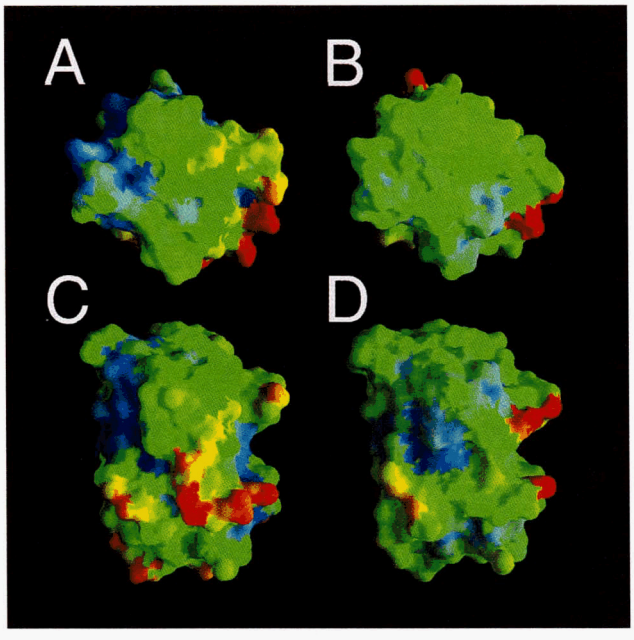


**Fig. 4.** Mappings of normalized *B*-factors on the solvent-accessible surface of Gly8Asp spinach Pc (**A**, **C**) and poplar Pc (**B**, **D**). The orientations are the same as in Figure 3. Color scale: blue, green, yellow, and red for low, medium, medium-high, and high *B*-factors, respectively. The plots were produced by GRASP (Nicholls et al., 1991).

dynamic in nature. As can be seen from Figure 4, the largest *B*-factors in both proteins are found in these regions, in particular in the lower acidic patch. Therefore, the details in the electrostatic potential may not be physiologically important since the side-chain conformations may adapt to optimize the interactions with the redox partners. Modifications of the charges of these side chains do result in lower reactivity, but the effects are moderate (Lee et al., 1995; Hibino et al., 1996; Hippler et al., 1996; Kannt et al., 1996; Young et al., 1997), possibly because of such structural adaptations. Neutralization of the upper acidic patch leads to a lower reactivity between cytochrome *f* and Pc when the latter originates from spinach (Kannt et al., 1996) compared to when it comes from *Silene pratensis* (Lee et al., 1995). The acidic residues in the 59–61 region are identical in the two proteins. However, Ser58 in spinach (and poplar) is replaced by a proline in *S. pratensis* and this may lead to different dynamic properties of the neighboring residues.

The situation is different for the hydrophobic patch. Judging from the *B*-factors, this region is quite rigid (Fig. 4A,B) and mutations in this area lead to strong impairment of the photosystem 1 reactivity, in particular for changes at positions 10 and 12 (Nordling et al., 1991; Haehnel et al., 1994; Sigfridsson et al., 1996). It is therefore conceivable that the binding between Pc and photosystem 1 at this hydrophobic interface requires a precise surface complementarity to maximize the van der Waals interactions and that there is little room for conformational adaptation. The same may be true for the interaction between Pc and cytochrome *f*. A recent NMR study (Ubbink et al., 1998) and electrostatic calculations (Pearson et al., 1996; Ullman et al., 1997) suggest that the active complex involves a close contact between the hydrophobic patch and the heme area on cytochrome *f*.

### *Conclusions*

Although the successful interplay between structural analyses and other biochemical studies has greatly advanced our understanding of the functional mechanism of Pc, a number of important questions remain to be answered. For example, what is the exact electron transport route through the protein and how are the dynamics of the different parts of the protein related to the efficiency of the electron transfer.

The current structural data of the Gly8Asp mutant of spinach Pc show that the two Pc structures from spinach and poplar are indeed very similar. Using the structure of the poplar Pc as a model in interpretation of the biochemical results obtained from spinach Pc may to a large extent be valid. However, to fully understand the results from the biochemical characterization of the numerous mutants of spinach Pc, more structural information is needed. In addition, investigations are underway to further study the dynamic behavior of the Cu atom, as well as study the influence of pH and the redox-state of the Cu atom in regards to the geometry around the Cu site.

## Materials and methods

### *Expression and purification*

Using the vector pUG101$t_r$ (Nordling et al., 1991), the mutant Gly8Asp was constructed using the polymerase chain reaction as reported in Landt et al. (1990), with the modifications described in Nordling et al. (1991). After sequencing on an Automated Laser Fluorescence (ALF) sequencer, the correct clone was expressed under the *lac* promoter, as described in Ejdebäck et al. (1997). Briefly, a periplasmic preparation was performed after 16–20 h of cultivation, followed by a pH precipitation. The resulting solution was loaded onto an anionic-exchange column after filtering and the blue Pc was eluted with a salt gradient. The sample was then concentrated against dry polyethylene glycol 20000 and gel filtrated, with 100 mM Tris-HCl (pH 7.5), 150 mM NaCl as the running buffer. The blue fraction of Pc was then oxidized by the addition of an excess of potassium ferricyanide, which was subsequently removed by passing the mixture through a Fast Desalting Column (Pharmacia, Uppsala, Sweden) on a Pharmacia FPLC system. Equilibration and elution buffer was 20 mM Tris-HCl (pH 8.0). Oxidized holo-protein was separated from reduced protein, apo-protein, and zinc-containing protein on a Resource Q anion-exchange FPLC column (Pharmacia), equilibrated with 20 mM Tris-HCl (pH 8.0), and eluted with a linear gradient of 0–250 mM NaCl, 20 mM Tris-HCl (pH 8.0) (Ejdebäck et al., 1997).

### *Biochemical and biophysical characterization*

The isoelectric point was measured as reported before (Sigfridsson et al., 1996). Briefly the sample was run on a self-hydrated Phast System Dry IEF gel, upon which a pH gradient from 3.5 to 5 was applied. Along each side of the gel, a marker sample was run with five samples ranging from 3.50 to 5.55. After the run, the gel was dyed with Coomassie Blue and scanned with a Pharmacia Phast Image system.

Reduction potentials, optical absorption and EPR spectroscopy, and electron-transfer kinetics were determined as earlier described (Sigfridsson et al., 1997).

**Table 2.** *Data collection and processing*

| | Data 1 | Data 2 |
|---|---|---|
| Space group | $P3_121$ | $P3_121$ |
| Unit cell parameters | | |
| $a = b$ (Å) | 75.519 | 75.582 |
| $c$ (Å) | 32.593 | 32.707 |
| $\alpha = \beta, \gamma$ (°) | 90.0, 120.0 | 90.0, 120.0 |
| Resolution range | 30.0–1.7 Å | 30.0–1.7 Å |
| Number of reflections | 12,009 | 11,977 |
| Completeness | | |
| 30.0–1.70 Å | 99.8% | 99.0% |
| 1.76–1.70Å | 98.0% | 91.3% |
| $I > 3\sigma(I)$ | | |
| 30.0–1.70 Å | 78.0% | 85.2% |
| 1.76–1.70 Å | 28.6% | 48.4% |
| $R_{merge}$[a]/average multiplicity | 0.059/9 | 0.052/9 |

[a] $R_{merge} = \Sigma_h \Sigma_i (I(h,i) - \langle I(h) \rangle) / \Sigma_h \Sigma_i (h,i)$ where $I(h,i)$ is the intensity value of the $i^{th}$ measurement of $h$ and $\langle I(h) \rangle$ the corresponding mean value of $h$ for all $i$ measurements of $h$.

*Crystallization and data collection*

Crystals of the mutant were obtained from 35% PEG 4000, 100 mM Na-acetate (pH 4.4), 0.2–0.3 M $MgCl_2$ at room temperature. After a few days rod-shaped crystals appeared with a typically hexagonal cross section of 0.3 mm. Data collection was performed at 24 °C on a Raxis-IIc imaging plate detector, and X-ray radiation (Cu $K_\alpha$) was produced by a Rigaku rotating anode generator (RU200) operating at 50 kV/100 mA. The crystal-to-detector distance was set to 80 mm and $2\theta$ to 0°. The data were collected in 2.0° oscillation steps covering 180° in spindle rotation. The data were processed and scaled using the programs Denzo and Scalepack (Otwinowski & Minor, 1996). Two crystals grown from the same droplet were used to collect diffraction data. Each of the two crystals yielded nearly complete data sets, Data 1 and Data 2, respectively (see Table 2). Merging the two data sets together gave a marginal increase in the overall $R_{merge}$ (1%), which indicates that the sets are virtually identical.

*Crystallographic refinement*

Crystallographic refinement was performed using the program X-PLOR (Brünger, 1992) and CCP4 suite (Collaborative Computational Project, Number 4, 1994). Molecular replacement was performed with the program AMoRe (Navaza, 1994) using the structure of poplar Pc (Protein Data Bank, entry code: 1plc) as a search model. The correct solution was verified by inspecting the resulted electron density map, which corresponded to the top solution from both rotation search and translation search, respectively. The top solution from rotation search (resolution 15–3 Å) is $4.8\sigma$ (second highest is $3.9\sigma$) above the mean, while the top solution from translation search (resolution 15–2.5 Å) has correlation coefficient (CC)/$R$-factor of 0.535/0.437 (0.346/0.513 for the next solution). Rigid body refinement brought the CC/$R$-factor to 0.589/0.436 (0.421/0.507 for the next solution). All the residues unique to poplar Pc were changed to the corresponding residues in the Gly8Asp mutant of the spinach protein and their rotamers adjusted, based on the electron density before any refinement. The initial refinement was done with Data 2 using X-PLOR.

The first round of simulated annealing (starting from 4,000 K) yielded an $R/R_{free}$ of 0.272/0.367 using data between 7.0 and 2.4 Å resolution (data with $I/\sigma(I) > 2$). Five rounds of simulated annealing were carried out with model building following each round, including the addition of solvent molecules based on electron density and plausible hydrogen bonding partners. The high resolution limit was gradually extended to 1.7 Å. Subsequent refinement was carried out on both data sets separately, and the test flag used for cross-validation was transferred from Data 2 to Data 1. After simulated annealing refinement, the program REFMAC (Murshudov et al., 1997) was used for further refinement, which included bulk solvent correction. Multiple cycles geometry restrained maximum likelihood refinement, including all data between 20 Å and 1.6 Å (anisotropic scaling was used for the last six cycles), resulted in a current $R/R_{free}$ of 0.183/0.204 for Data 2 (0.183/0.211 for Data 1). Program O (Jones et al., 1991) was used for the graphical modeling of the structure. The RMS difference for $C_\alpha$ atoms between the models based on the two data sets is 0.04 Å. Only the refined model from Data 2 (since the refinement using Data 2 yielded a better $R_{free}$ value) was used in the continued structural analysis and comparisons with other structures as presented in this paper.

In the second phase of refinement, the model building was based on maps calculated using $\sigma_A$-weighted coefficients. If not stated otherwise, all maps mentioned are those calculated with the $\sigma_A$-weighted coefficients from REFMAC. Superposition of different structure models was done either inside program O or using program LSQMAN (Kleywegt, 1996). Reference atoms in least-squares fittings were $C_\alpha$ atoms from all residues constituting the core $\beta$-structure of the protein. In the discussions, "shifts," "movements," and "displacements" all refer to differences between the structures of spinach and poplar Pc after superposition.

## Acknowledgments

We thank Drs. Lennart Sjölin and Tore Vänngård for their help and support in this project, in particular Lennart Sjölin, for help in the initial crystallization trials on the wild-type protein, and Tore Vänngård for critical reading of the manuscript. We also thank Anders Bergkvist, Charlotta Johansson, and Dr. Göran Karlsson for sharing their results from the NMR structure determination of spinach Pc. Dr. Vratislav Langer is thanked for technical support during data collection. This work was supported by grants from the Swedish Natural Science Research Council.

## References

Badsberg U, Jørgensen AMM, Gesmar H, Led JJ, Hammerstad JM, Jespersen L, Ulstrup J. 1996. Solution structure of reduced plastocyanin from the blue-green alga *Anabaena variabilis*. *Biochemistry 35*:7021–7031.

Bagby S, Driscoll PC, Harvey TS, Hill HAO. 1994. High-resolution solution structure of reduced parsley plastocyanin. *Biochemistry 33*:6611–6622.

Brünger AT. 1992. *X-PLOR. Version 3.1. A system for X-ray crystallography and NMR*. New Haven, CT: Yale University.

Chapman GV, Colman PM, Freeman HC, Guss JM, Murata M, Norris VA, Ramshaw JAM, Venkatappa MP. 1977. Preliminary crystallographic data for a copper-containing protein, plastocyanin. *J Mol Biol 110*:187–189.

Collaborative Computational Project, Number 4. 1994. *Acta Cryst D50*:760–763.

Colman PM, Freeman HC, Guss JM, Murata M, Norris VA, Ramshaw JAM, Venkatappa MP. 1978. X-ray crystal structure analysis of plastocyanin at 2.7 Å resolution. *Nature 272*:319–324.

Durell SR, Labanowski JK, Gross EL. 1990. Modeling of the electrostatic potential field of plastocyanin. *Arch Biochem Biophys 277*:241–254.

Ejdebäck M, Young S, Samuelsson A, Karlsson BG. 1997. Effects of codon

usage and vector-host combinations on the expression of spinach plastocyanin in *Escherichia coli*. *Protein Exp Purif 11*:17–25.
Evans SV. 1993. SETOR: Hardware lighted three-dimensional solid model representations of macromolecules. *J Mol Graphics 11*:134–138.
French GS, Wilson KS. 1978. On the treatment of negative intensity observations. *Acta Cryst A34*:517–525.
Gross EL. 1993. Plastocyanin: Structure and function. *Photosynth Res 37*:103–116.
Guss JM, Bartunik HD, Freeman HC. 1992. Accuracy and precision in protein structure analysis: Restrained least-squares refinement of the structure of poplar plastocyanin at 1.33 Å resolution. *Acta Cryst B48*:790–811.
Haehnel W, Jansen T, Gause K, Klösgen RB, Stahl B, Michl D, Huvermann B, Karas M, Herrmann RG. 1994. Electron transfer from plastocyanin to photosystem I. *EMBO J 13*:1028–1038.
Hibino T, Lee BH, Yajima T, Odani A, Yamauchi O, Takabe T. 1996. Kinetic and cross-linking studies on the interactions of negative patch mutant plastocyanin from *Silene pratensis* with photosystem I complexes from cyanobacteria, green algae, and plants. *J Biochem 120*:556–563.
Hippler M, Reichert J, Sutter M, Zak E, Altschmied L, Schröer U, Herrmann RG, Haehnel W. 1996. The plastocyanin binding domain of photosystem I. *EMBO J 15*:6374–6384.
Jones TA, Zou JY, Cowan SW, Kjeldgaard M. 1991. Improved methods for building protein models in electron density maps and the location of errors in these models. *Acta Cryst A47*:110–119.
Kannt A, Young S, Bendall DS. 1996. The role of acidic residues of plastocyanin in its interaction with cytochrome *f*. *Biochim Biophys Acta 1277*:115–126.
Kleywegt GJ. 1996. Use of non-crystallographic symmetry in protein structure refinement. *Acta Cryst D52*:842–857.
Landt O, Grunert HP, Hahn U. 1990. A general method for rapid site-directed mutagenesis using the polymerase chain reaction. *Gene 96*:125–128.
Laskowski RA, MacArthur MW, Moss DS, Thornton JM. 1993. PROCHECK: A program to check the stereochemical quality of protein structures. *J Appl Cryst 26*:283–291.
Lee BH, Hibino T, Takabe T, Weisbeek PJ. 1995. Site-directed mutagenetic study on the role of negative patches on silene plastocyanin in the interactions with cytochrome *f* and photosystem I. *J Biochem 117*:1209–1217.
Murshudov GN, Vagin AA, Dodson EJ. 1997. Refinement of macromolecular structures by the maximum-likelihood method. *Acta Cryst D53*:240–255.
Navaza J. 1994. AMoRe: An automated package for molecular replacement. *Acta Cryst D50*:157–163.
Nicholls A, Sharp K, Honig B. 1991. Protein folding and association: Insights from the interfacial and thermodynamic properties of hydrocarbons. *Proteins Struct Funct Genet 11*:281–296.
Nordling M, Sigfridsson K, Young S, Lundberg LG, Hansson Ö. 1991. Flash-photolysis studies of the electron transfer from genetically modified spinach plastocyanin to photosystem I. *FEBS Lett 291*:327–330.
Otwinowski Z, Minor W. 1996. Processing of X-ray diffraction data collected in oscillation mode. *Methods Enzymol 276*:307–326.
Pearson DC Jr, Gross EL, David ES. 1996. Electrostatic properties of cytochrome *f*: Implications for docking with plastocyanin. *Biophys J 71*:64–76.
Redinbo MR, Cascio D, Choukair MK, Rice D, Merchant S, Yeates TO. 1993. The 1.5-Å crystal structure of plastocyanin from the green alga *Chlamydomonas reinhardtii*. *Biochemistry 32*:10560–10567.
Redinbo MR, Yeates TO, Merchant S. 1994. Plastocyanin: Structural and functional analysis. *J Bioenerg Biomembr 26*:49–66.
Romero A, De la Cerda B, Varela PF, Navarro JA, Hervás M, De la Rosa MA. 1998. The 2.15 Å crystal structure of a triple mutant plastocyanin from the cyanobacterium *Synechocystis* sp. PCC 6803. *J Mol Biol 275*:327–336
Sigfridsson K, Young S, Hansson Ö. 1996. Structural dynamics in the plastocyanin-photosystem 1 electron-transfer complex as revealed by mutant studies. *Biochemistry 35*:1249–1257.
Sigfridsson K, Young S, Hansson Ö. 1997. Electron transfer between spinach plastocyanin mutants and photosystem 1. *Eur J Biochem 245*:805–812.
Tröger W, Lippert C, Butz T, Sigfridsson K, Hansson Ö, McLaughlin E, Bauer R, Danielsen E, Hemmingsen L, Bjerrum, ISOLDE Collaboration. 1996. Small scale intramolecular flexibility in $^{111m}$Cd-plastocyanin. *Z Naturforsch 51A*:431–436.
Ubbink M, Ejdebäck M, Karlsson BG, Bendall DS. 1998. The structure of the complex of plastocyanin and cytochrome *f*, determined by paramagnetic NMR and restrained rigid-body molecular dynamics. *Structure 6*:323–335.
Ullman GM, Knapp EW, Kostic NM. 1997. Computational simulation and analysis of dynamic association between plastocyanin and cytochrome *f*. Consequences for the electron-transfer reaction. *J Am Chem Soc 119*:42–52.
Young S, Sigfridsson K, Olesen K, Hansson Ö. 1997. The involvement of the two acidic patches of spinach plastocyanin in the reaction with photosystem 1. *Biochim Biophys Acta 1322*:106–114.